Pulsed NMR

James Amarel, Adeel Ali, and Dr. Matt Moelter

May 15, 2017

1 Goal

To observe the spin echo in pulsed NMR techniques and measure the relaxation times associated with field non-uniformity, spin-lattice interaction, and spin-spin coupling of protons in mineral oil and glycerin.

2 Introduction/Background

In the presence a magnetic field B_o, the magnetic moment of the proton has access to an aligned and anti-aligned state, so photons of energy on resonance with the transition energy for spin flips

$$\Delta E = g\mu_N B_o \tag{1}$$

where $g = 5.5857$ is the g-factor for the proton and $\mu_N = 5.05 \times 10^{-27}$ J/T is the nuclear magneton, can stimulate transitions between states. For a collection of atoms in thermal equilibrium with an external magnetic field B_o, the ratio of spin-down protons to spin-up protons can be found from statistical mechanics by taking the ratio of the Boltzmann factors of each state

$$\frac{N_-}{N_+} = \frac{e^{-E_-/k_bT}}{e^{-E_+/k_bT}} = e^{-\Delta E/kT} \tag{2}$$

where E_- and E_+ are the energies of the spin down (anti-aligned) and spin up (aligned) states, respectively, where the difference $\Delta E = E_- - E_+$ forms Equation 1. At temperature 300 K and for the typical magnetic field strengths applied in this experiment of 3.5 T, $\Delta E \ll k_bT$, thus, $\frac{N_-}{N_+} = 0.99997$, therefore, the spin up/down states are not quite equally populated. This imbalance is described by a nonzero net magnetization $\boldsymbol{M}$, which is the vector sum of all proton magnetic moments, and is parallel to $\boldsymbol{B}_0$ when the sample is in thermal equilibrium. In the frame rotating with the proton spin, which precesses around $\boldsymbol{B}_0$ at frequency $f_o = \Delta E/h$, where h is Planck's constant, an RF field of frequency f_o applied perpendicular to $\boldsymbol{M}$ will appear stationary, which results in the precession of $\boldsymbol{M}$ about $\boldsymbol{B}_{RF}$ [1]. For an RF pulse of width t_w, $\boldsymbol{M}$ precesses through the angle

$$\theta = \frac{2\pi g\mu_N B_{RF} t_w}{h} \tag{3}$$

which allows manipulation of the precession angle between $\boldsymbol{M}$ and $\boldsymbol{B}_o$ (e.g. a 90^o pulse requires pulse width $t_{90} = h/4g\mu_N B_{RF}$).

Magnetic interactions between neighboring spins is weak, but produces a local variation in the magnetic interactions experienced by each spin. Consequently, no two spins precess at exactly the same frequency. Therefore, following a 90^o pulse applied to a system in thermal equilibrium, $\boldsymbol{M}$ is rotated so that it is precessing in the plane perpendicular to $\boldsymbol{B}_o$, then there is decoherence of spins to the spin-spin interactions, resulting in the strength of $\boldsymbol{M}$ being reduced in an exponential manner, which is characterized by the time constant T_2. The net magnetization also decays due to external magnetic field non-uniformity, which again causes the protons to precess at different rates. This process occurs on the microsecond scale, since spins precess at $\approx$ 15 MHz, if the magnetic field varies by 1% between two spins, they will be 180^o out of phase after approximately 300 μs. Additionally, the net magnetization is driven towards thermal equilibrium by interactions with its external environment, such as electrons and nucleons, which are called spin-lattice interactions with time constant T_1. The time constant for the net decay of $\boldsymbol{M}$ is called T_2^*.

3 Procedure and Data

In order to observe the decay of $\boldsymbol{M}$, we used a pair of coils in the plane perpendicular to $\boldsymbol{B}_o$ to detect a change in magnetic flux due to the motion of the component of $\boldsymbol{M}$ within the plane as an induced current, which decays with $\boldsymbol{M}$, as seen in Figure 1, in what is called free-induction decay (FID). Following a rotation away from the equilibrium state, $\boldsymbol{M}$ processes around $\boldsymbol{B}_o$ at angle θ determined by Equation 3. So the experimental task was to choose a pulse width such that $\boldsymbol{M}$ rotates to precess in the plane of the inductor coils, and then repeatedly apply this pulse at the highest frequency, while allowing the system to return to equilibrium before another pulse is applied.

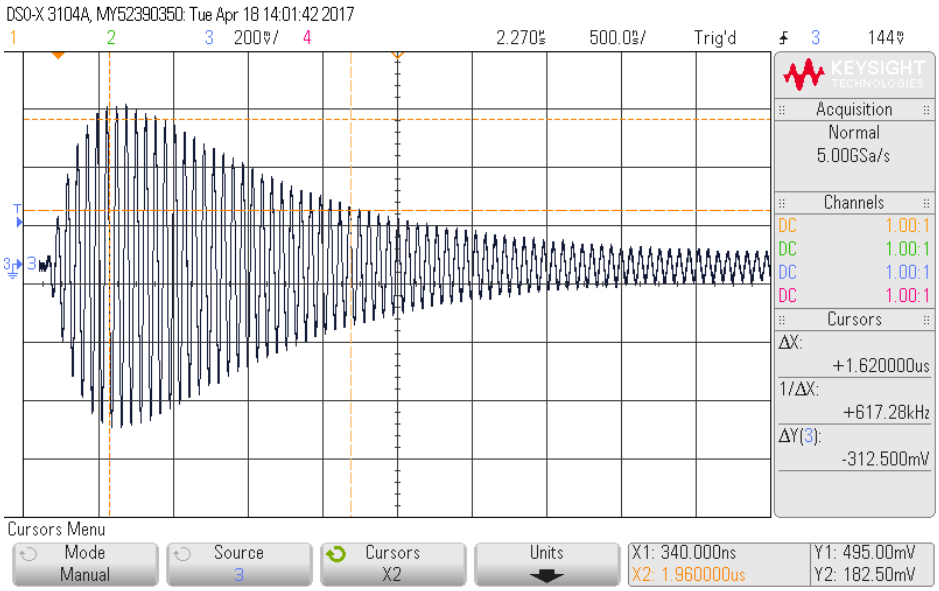

Figure 1: Free induction decay of the induced current for a vial containing mineral oil.

Note the FID is an AC signal due to the precession of $\boldsymbol{M}$. As seen in Figure 2, we

subject a sample vial to a static magnetic field $B_o = 3.5$ T via a permanent magnet housing, which contains the receiver used to amplify and detect the current induced by $\boldsymbol{M}$, and a coil that seats the sample and created $\boldsymbol{B}_{RF}$ when current from the RF amplifier passed through it.

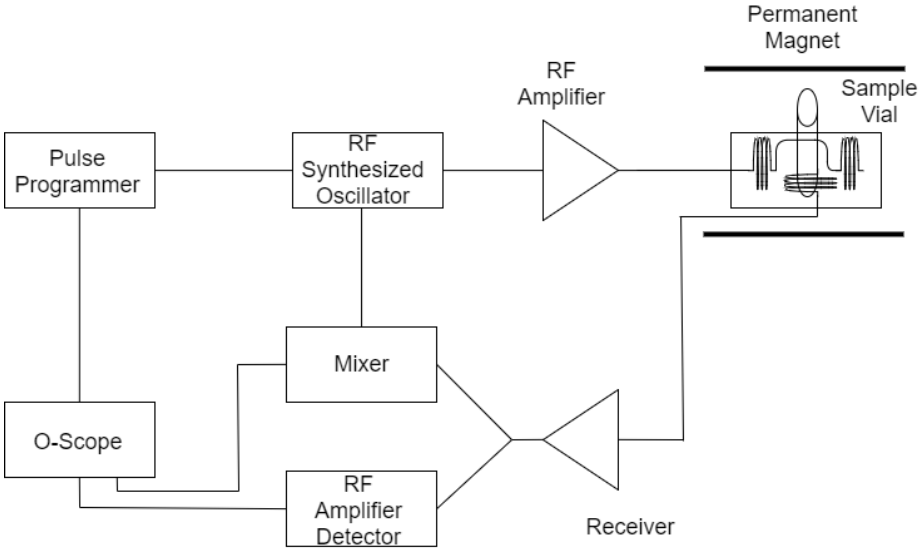

Figure 2: Block diagram of the experimental apparatus.

We used a frequency synthesizer to precisely generate an RF field of frequency $f_{RF} = 15.38214$ MHz, with strength $B_{RF} = 12$ gauss. The FID signal in Figure 1 oscillates at 15.3 MHz, in agreement with our choice for f_{RF}. The RF field was gated by a pulse programmer, which allowed for control of the parameters such as the number of pulses, pulse separation, repetition rate/time, and pulse width. An example of a single pulse output is seen in Figure 3.

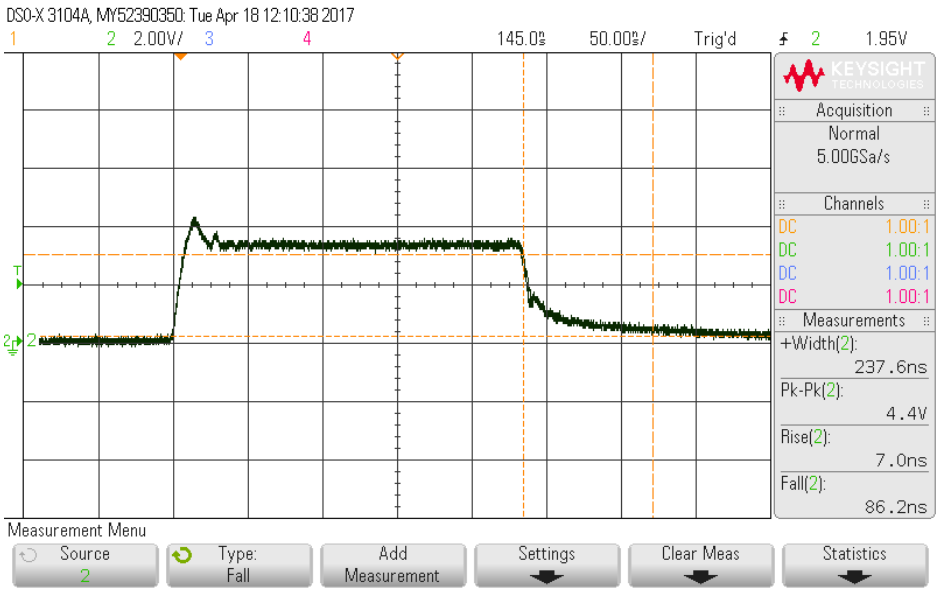

Figure 3: Oscilloscope display of the RF gate pulse.

We observed the induced current signal on an oscilloscope with the assistance of a rectifier circuit, which allowed for easy measurement of the time constants from a

decay envelope. The receiver also sent signal to a mixer, which we used to match f_{RF} to the natural procession frequency of the sample, by tuning the beat frequency to a minimum.

To produce the maximum amplitude FID signal for RF field strength $B_{RF} = 12$ gauss, we calculated the required pulse width for a 90 degree rotation $t_{90} = 4.52\ \mu s$. Tuning of t_{90} resulted in the optimal pulse width for maximum FID signal amplitude was 4.11 μs, which is a shorter pulse than calculated, suggesting the system is more readily manipulated. This phenomena may be due to the spins moving as a collection, and the spin lattice interactions as other spins experience torque due to B_{RF}.

An oscilloscope image of the rectified FID decay is seen in Figure 4, where we measured the net decay constant $T_2^* = 1.62\ \mu s$ as the e^{-1} point of the envelope. Since the signal decay is dominated by external magnetic field non-uniformity, we employ a trick to study only the decay due to spin-spin interactions. After applying a 90 degree pulse, $\boldsymbol{M}$ dephases as the spins precess due to magnetic interactions, so applying a 180 degree pulse at time delay τ after the 90 degree pulse, flips the spins such that at time τ after the 180 degree pulse, the spins meet in alignment. This realignment causes a bump in the FID signal following a period when $\boldsymbol{M}$ had dephased to magnitude zero and is called a spin echo.

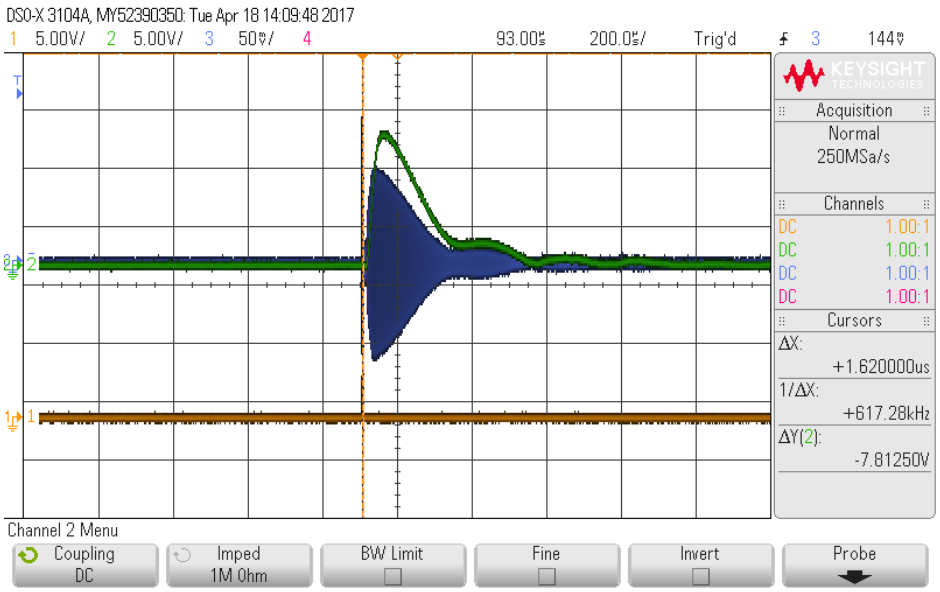

Figure 4: FID signal (blue).

The spin echo still carries the signature of spin-spin interaction - its amplitude is decreased in comparison with the original pulse - as the spins bump into each other no differently after the complete inversion. Thus the spin-spin dephasing is not reversed by the 180 degree pulse. We then built a 180 degree pulse of width 11.58 μs that followed at delay time τ from a primary 90 degree pulse of width 6.58 μs and adjusted the pulse delay τ until we found the point at which the echo amplitude decreased to e^{-1} of the initial amplitude. Here, τ provided an approximate measurement of the spin-spin relaxation time as $\tau \approx T_2 = 30 \pm 1\ ms$, where we have estimated a 1 ms uncertainty in our scope readings.

For an alternate measurement of T_2, we used nine 180 degree pulses in order to create multiple spin echoes, which, as seen in Figure 5, decay exponentially in amplitude

with time, the e^{-1} point of this decay is an estimate of T_2.

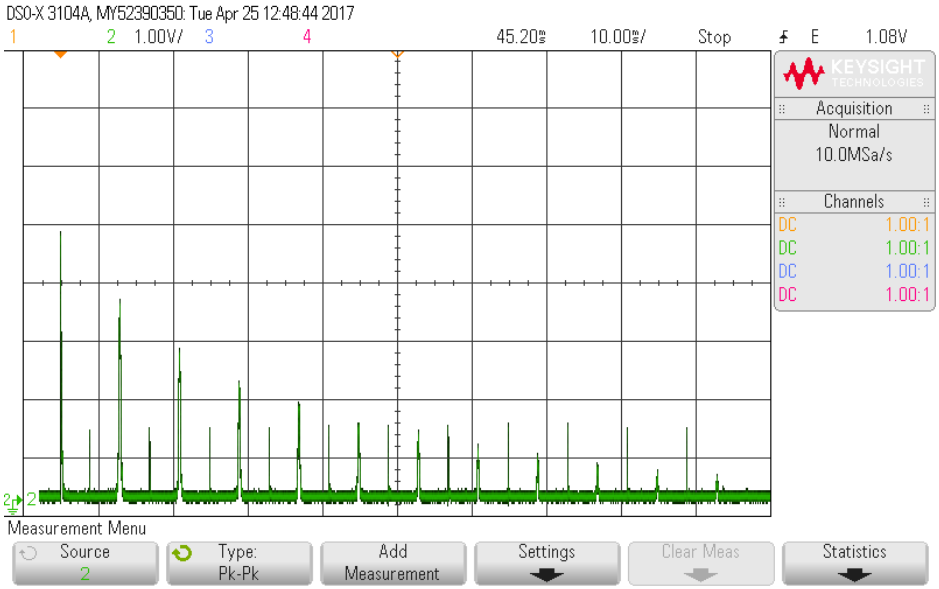

Figure 5: Exponential decay of a series of spin echoes, for a pulse sequence beginning with a 90 degree pulse, then a 180 degree pulse after τ, followed by a train of 180 degree pulses with spacing 2τ for a mineral oil sample.

In order to measure the characteristic decay time T_1 due to spin lattice interactions, we utilized another two-pulse sequence to measure the component of the magnetization within the detection plane, except in this case, we began with a 180 degree pulse, which was followed by a 90 degree pulse after delay τ. After the second pulse, $\boldsymbol{M}$ has been rotated entirely into the detection plane, but the magnitude of the FID signal still depends on τ due to ongoing spin-lattice interactions. By increasing the delay in 5 ms steps and recording the voltage of the FID signal, we find the delay time τ_o such that, following a 180 degree pulse away from equilibrium, $\boldsymbol{M}$ has decayed to magnitude zero. For delay times less than τ_o, $\boldsymbol{M}$ is inverted, and for delay times greater than τ_o, $\boldsymbol{M}$ is aligned with $\boldsymbol{B}_o$ and is being thermally driven towards equilibrium, so we expect the height of the FID signal to decrease in height for short τ, then begin increasing, eventually reaching a maximum, for long τ. This data is shown in Figure 6, which is an exponential rise, as the component of $\boldsymbol{M}$ evolves according to

$$M_z(t) = M_o(1 - 2e^{-t/T_1}) \tag{4}$$

where M_z is the component of $\boldsymbol{M}$ in the detection plane and M_o is the equilibrium magnitude. Note Equation 4 begins at $M_z = -M_o$ when $t = 0$, since the magnetization is completely inverted following a 180 degree pulse.

In Figure 6, we have introduced a negative sign to the FID amplitude for measurements at short τ, for which $\boldsymbol{M}$ was inverted. To ensure the validity of Equation 6, we increased the repetition time of the pulse sequences to 250 ms, such that the system had time to reach equilibrium before an additional pulse was applied, and the magnitude of $\boldsymbol{M}$ reached a constant maximum for large τ. We found a delay time of 22 ± 2 ms resulted in zero signal strength, which, from Equation 6, gives $T_1 = \tau/ln(2) = 32 \pm 2$ ms, which is significantly longer than $T_2^* = 1.6\ \mu s$, and also is greater than the spin-spin relaxation time.

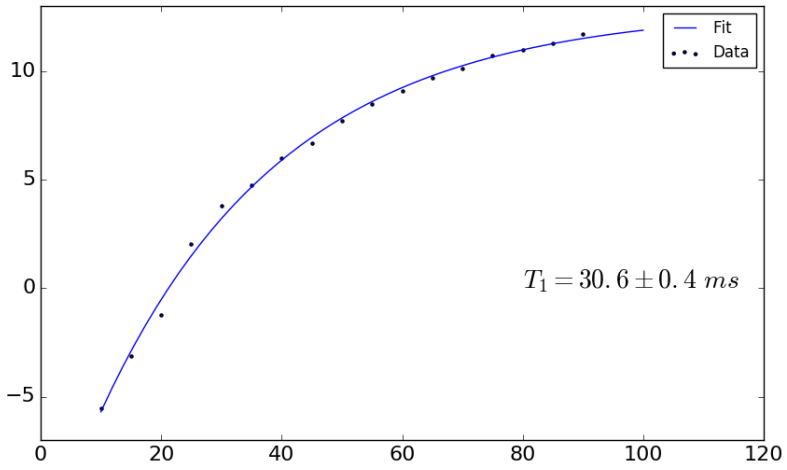

Figure 6: FID signal as a function of the delay time between a primary 180 degree pulse and a secondary 90 degree pulse for a mineral oil sample, with a numerical fit to Equation 4.

We also determined T_1 for a glycerin sample by determining the value of τ for which the FID signal is zero, where we found $\tau = 47 \pm 2$ ms, which gave $T_1 = 70 \pm 3$ ms.

4 Analysis and Discussion

In order to determine the value of T2 for both glycerol and mineral oil, we selected the peaks from Figure 5 that corresponded to a spin echo signal, which meant selecting every other peak, since the intermediary peaks are due to an imperfectly tuned 90 degree pulse. Then we performed an exponential fit to find the time constant of the decay of the spin echo signal height, which is shown in Figure 7 and Figure 8, for glycerol and mineral oil, respectively.

For convenience, Table 1 displays all the time constants we have measured, for both samples.

Table 1: Tabulated results of relaxation times.

Sample	T_2^*	T_1	T_2
Mineral Oil	1.62 μs	30.6 $\pm$0.04 ms	31.9 $\pm$ 0.7 ms
Glycerin		70 $\pm$ 3 ms	74.5 $\pm$1.9 ms

The time constant T_2^* representing the net decay is orders of magnitude shorter than both T_1 and T_2, signifying that general thermal fluctuations are overwhelmingly dominant over the relaxation processes that are the result of spin-lattice interactions (T_1) and spin-spin interactions (T_2). The fact that T_1 and T_2 occur on the same time scale suggests that the influence of all the proton spins on each other has a nearly equivalent effect on the net magnetization as does the interactions between the protons and all the other lattice entities (such as electrons, nucleons, and impurities).

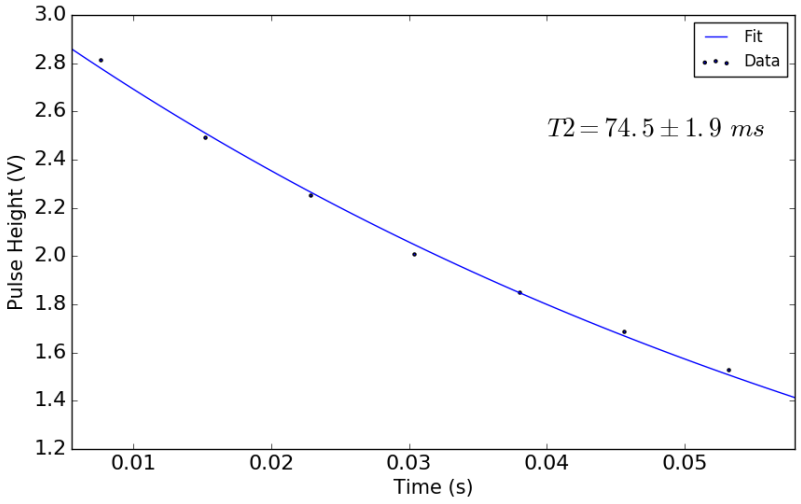

Figure 7: Exponential fit to the decaying spin echo signal height for protons of a glycerol sample, which yields the spin-spin relaxation time constant T2.

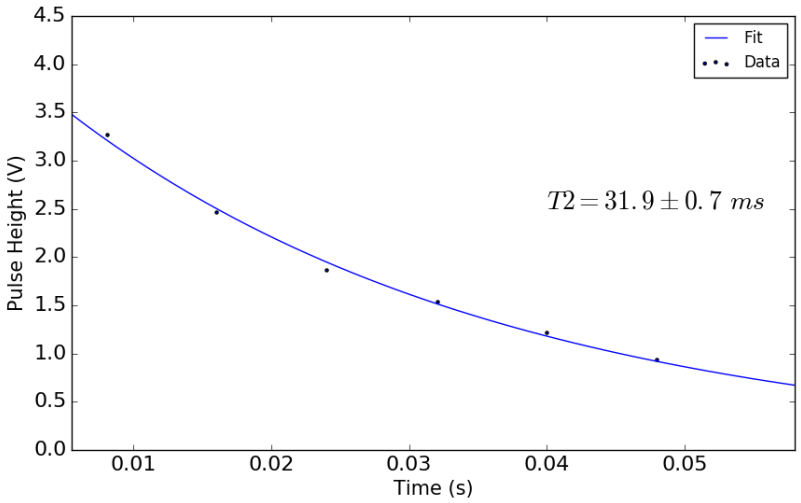

Figure 8: Exponential fit to the decaying spin echo signal height for protons of a mineral oil sample, which yields the spin-spin relaxation time constant T2.

If we were to assume the electron influence is negligible, then the strength of both each nucleon interaction is equivalent. Otherwise, the protons are coupling to each other more strongly than they are coupling to the neutrons, which are both spin 1/2 particles.

5 Conclusion

We used pulsed NMR techniques to reorient the net magnetization vector of proton spins within a sample of glycerin and mineral oil. Reorientation was the result of applying an RF magnetic field pulse, which exerted a torque on each proton spin within the sample, since those spins were prepared to be processing about a constant and uni-

form external magnetic field. By reorienting the magnetization vector within the plane of two inductor coils, we measured its magnitude through free induction decay, which occurs due to the changing magnetic field that accompanies a precessing field vector. By utilizing a sequence of reorientation pulses, we were able to measure the relaxation rates T_2^*, T_1, and T_2 of our samples. We found that the net decay T_2^* was overwhelmingly strong and masked the physics of spin-spin coupling and spin-lattice interactions. In ordered to remove the noise due to magnetic field inhomogeneities, we allowed the spins to dephase for a delay time τ, before inverting them completely with a 180 degree pulse, which caused them to evolve backwards, towards an aligned state, called a spin echo, although with a decreased net magnetization, which was the byproduct of spin-lattice interactions. Then, in order to measure the spin-spin relaxation time, we applied a 180 degree pulse to invert the system into a state aligned with the external magnetic field. In this case, the net magnetization evolves towards its equilibrium state, and crosses a zero point along the way. We then measured an approximate relaxation rate for this process by periodically moving the magnetization vector into the inductor plane while allowing it to evolve away from its non-equilibrium state. We found that relaxation due to spin-spin coupling occurred on a similar timescale as that due to spin-lattice interactions, which were both on the order of 50 ms.

References

[1] Adrian C. Melissinos. *Experiments in Modern Physics.* Academic Press, 2003.